EARTH SURFACE PROCESSES AND LANDFORMS
Earth Surf. Process. Landforms **39**, 2002–2015 (2014)

Published online 24 May 2014 in Wiley Online Library
(wileyonlinelibrary.com) DOI: 10.1002/esp.3595

The normalized topographic method: an automated procedure for gully mapping using GIS

Carlos Castillo,[1,2]* Encarnación V. Taguas,[2] Pablo Zarco-Tejada,[1,3] Mike R. James[4] and Jose A. Gómez[1]
[1] Institute for Sustainable Agriculture-CSIC, Cordoba, Spain
[2] Department of Rural Engineering, University of Cordoba, Cordoba, Spain
[3] European Commission, Joint Research Centre, Institute for Environment and Sustainability, Ispra, Italy
[4] Lancaster Environment Centre, Lancaster University, Lancaster, UK

Received 14 June 2013; Revised 15 April 2014; Accepted 16 April 2014

*Correspondence to: Carlos Castillo, Institute for Sustainable Agriculture-CSIC. Apartado 4084. 14080 Cordoba Spain. E-mail: ccastillo@ias.csic.es

ESPL
Earth Surface Processes and Landforms

ABSTRACT: Gully delineation is a critical aspect of accurately determining soil losses but associated methodologies are rarely detailed. Here, we describe a new gully mapping method, the normalized topographic method (NorToM), based on processing digital elevation model (DEM) data, and we assess associated errors when it is applied over a range of geomorphological scales. The NorToM is underpinned by two gully detection variables (normalized slope and elevation) calculated over local windows of prescribed size, and a group of filtering variables. For four study sites, DEMs of gullies were obtained using field and airborne photo-reconstruction and evaluated using total station and differential global positioning system (dGPS) survey. NorToM provided accurate areal and volume estimates at the individual gully scale but differences increased at the larger gully system and gully network scales. We were able to identify optimal parameters for using the NorToM approach and so confirm that is represents a useful scale-independent means of gully mapping that is likely to be valid in other environments. Its main limitations are that the normalization process might be time-consuming at regional scales and the need for a fixed window size when applied to landforms with extreme variations in dimensions. Copyright © 2014 John Wiley & Sons, Ltd.

KEYWORDS: gully erosion; mapping; resolution; GIS; photo-reconstruction; DEM

Introduction

In many environments gully erosion is one of the main processes causing soil degradation (Poesen *et al.*, 2003; De Santisteban *et al.*, 2006). Assessing soil losses usually involves the delineation of gully perimeter and the calculation of gully volume. Conventional and more sophisticated innovative techniques have been used for this purpose (e.g. Casalí *et al.*, 1999; James *et al.*, 2007; Giménez *et al.*, 2009, Evans and Lindsay, 2010); however, little discussion is usually provided about the criteria for gully delineation and their implications for measurements error. To our knowledge there are no specific studies that assess where gullies 'begin' in the transverse direction (i.e. perpendicular to the gully length) while, at the same time, this determination is an unavoidable step to obtain accurate volume estimates. Moreover, developing consistent protocols for defining gully limits would be desirable to make measurements comparable between different techniques (Castillo *et al.*, 2012).

Typically, gully limits are defined using field observations (Casalí *et al.*, 2006; Wu *et al.*, 2008b; Perroy *et al.*, 2010), aerial photography interpretation (Gómez-Gutiérrez *et al.*, 2009) or analysis of topographic parameters from digital elevation models (DEMs, Daba *et al.*, 2003). More recently, several studies have described methods for mapping gully networks using semi-automated or fully automated approaches based on digital terrain analysis (Evans and Lindsay, 2010; Perroy *et al.*, 2010) or object-oriented classification (Eustace *et al.*, 2011; Shruthi *et al.*, 2011; Johansen *et al.*, 2012) using LiDAR (light detection and ranging) or spaceborn high resolution data (0.5 m to 2 m resolutions). These approaches require the definition of a rule-set, an array of sequential algorithms and thresholds to detect gully presence and identify gully extents. Such techniques proved to be advantageous at the landscape scale when compared with time-consuming and subjective manual delineation methods. Nevertheless, they rely on the definition of thresholds in absolute terms and values are not likely to be applicable to other regions. In addition, the rules given are not often very intuitive since they comprise a combination of topographical and image parameters that are not always directly related to gully features. A fully automated procedure, scale-independent and solely dependent on meaningful topographic variables would be helpful in mitigating many of these drawbacks.

Resolution plays a major role in the analysis of DEMs and the accuracy of their derivatives (Thompson *et al.*, 2001; Zandbergen, 2006; Wu *et al.*, 2008a). Previous works have argued that there may be a compromise between the accuracy obtained and the amount of data handled (Zhang and Montgomery, 1994; Hancock, 2005). This is a relevant question in a context characterized by the increasing development of high-resolution datasets and the subsequent challenge of efficient data management. At the other extreme, when only coarse resolutions are available and automated procedures are carried out, resampling the original DEMs to smaller pixel sizes to increase accuracy should be evaluated. The performance of gully delineation algorithms is likely to be affected by edge effects, which are sensitive to cell dimensions, regardless of the quality of the data collected.

The main aim of this study is to describe an automated, normalized topographic method (NorToM) for gully delineation, that uses geographic information system (GIS) algorithms and topographic data, and to evaluate its performance across a range of scales (from rill to badlands). For this purpose it is necessary to (i) first describe the automated routines, and explore the optimal intervals of the key parameters; (ii) evaluate the procedure accuracy at the rill and gully scales, as a function of DEM resolution; (iii) finally assess its performance at large gully and badland scales, by comparison with the results from a manual gully delineation method.

Material and Methods

Study areas

To evaluate the performance of NorToM, four study areas were considered in order to cover a range of gradually increasing geomorphological scales, from rill to badland areas, in Spain: Santa Cruz (rill-ephemeral gully, REG), Galapagares (permanent gully, PG), Fuentsanta (large gully system, LG) and Belerda (badland landscape, BL). The Santa Cruz and Galapagares areas are representative of the Campiña, a rolling landscape in the Guadalquivir River Valley covered, mainly, with field crops (bean, sunflower and wheat) on Vertisol soils under the FAO classification. Figure 1 and Table I show the characteristics of the study sites and the properties of the associated datasets.

At the Santa Cruz site (20 km south of Córdoba, 37°44′17.53" N, 4°37′52.30" W) a REG was surveyed in an olive grove using field three-dimensional (3D) photo-reconstruction (22-m-long main channel, average width W_{av} of 0.9 m and average depth H_{av} of 0.2 m). This site was selected because of its challenging topography. It is characterized by a changing geometry and shallow depth, sharing features both of rill and ephemeral gully ($H_{av} < 0.3$ m, $W_{av} > 0.5$ m, maximum width $W_{max} = 2$ m). The reference perimeter was defined by visual identification of the change in slope at the top of the gully walls (i.e. the point where the relatively flat gully margins starts to slope into the gully) and its coordinates measured using a total station (Topcon GTS-210).

At the Galapagares site (15 km south-east of Córdoba, 37 49´ 9´´N, 4 35´ 39´´W) a DEM of 400-hectares of annual crops under intensive agricultural practices was obtained in an airborne photograph campaign in December 2012. One PG (Figures 1b and 1c) was selected (a 662 m-long main channel, $W_{av} \sim 10$ m, $W_{max} \sim 20$ m). The gully perimeter was delineated through a field survey, using the visual change-in-slope criterion and a centimetre-accurate differential global positioning system (dGPS).

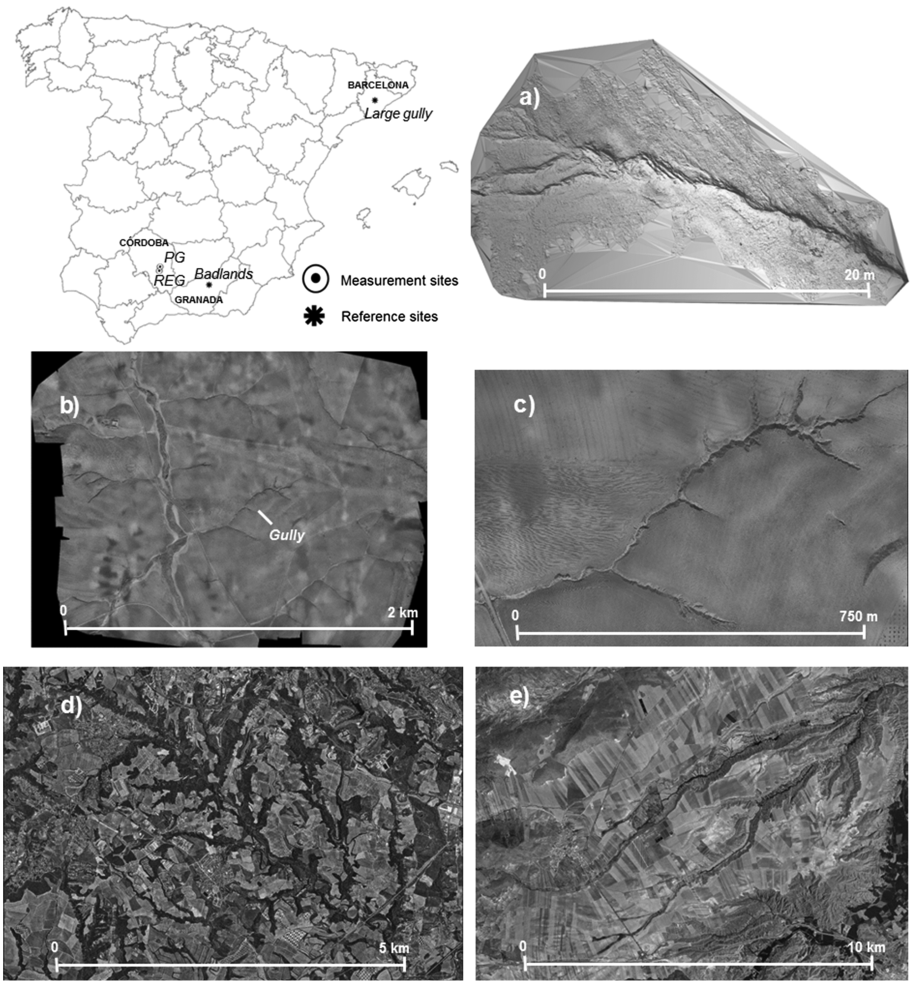

Figure 1. Study sites, scale and method: (a) Santa Cruz, rill-ephemeral scale (REG), DEM from 3D photo-reconstruction; (b) Galapagares area, orthophotography from airborne campaign; (c) Galapagares, permanent gully (PG) scale, orthophotography from airborne campaign; (d) Fuentsanta, large gully scale (LG), orthophotography from Instituto Geográfico Nacional (CNIG, 2013); (e) Belerda, badland scale (BL), orthophotography from Instituto Geográfico Nacional (CNIG, 2013).

Table I. Description of the study sites and dataset properties

Site	Scale	Extent	W_{av} (m)	H_{av} (m)	DEM source	Original resolution (m)	Reference method	Land use	Location
Santa Cruz	Rill/Ephemeral gully (REG)	400 m^2	0.9	0.2	3D photo-reconstruction	0.020	Total station	Olive orchard	Córdoba, Spain
Galapagares	Permanent gully (PG)	30 ha	10.6	3.4	Airborne reconstruction	0.066	Differential GPS	Field Crops	Córdoba, Spain
Fuentsanta	Large gully (LG)	25 km^2	153.5	23.6	Airborne LiDAR (CNIG, 2012)	5.000	Manual delineation	Vineyards, winter cereals and urban areas	Penedès, Barcelona, Spain
Belerda	Badland (BL)	90 km^2	437.6	57.8	Airborne LiDAR (CNIG, 2012)	5.000	Manual delineation	Rangeland, cereal fields, olive and almond plantations	Guadix, Granada, Spain

Note: H_{av}, average gully depth; W_{av}, average gully width.

To assess the NorToM performance at larger scales, firstly, a gully network, the Fuentsanta gully system, in the Pénedes region was evaluated (LG, Barcelona, Spain, 41°29′5.72" N, 1°48′57.16" E). This area was previously studied by Martínez-Casasnovas *et al.* (2002) for assessment of sediment production. The main land use is vineyards and winter cereals with presence of grassland, shrublands, forested lands and urbanized areas. Secondly, the badland scale was represented by an area including the Belerda 'barranco' (BL, Guadix, Granada, 37°21′36.77"N, 3°14′44.64" W, previously studied by Marzolff *et al.*, 2011) covered with cereal fields, olive and almond plantations.

The influence of vegetation on gully delineation is not addressed specifically, although it is believed to be minor in this study because (i) vegetation was negligible at the REG scale, (ii) very reduced at the Galapagares site (an intensively cultivated area), and (iii) vegetation height was small relative to the gully depth at the Fuentsanta and Belerda gullies.

Dataset description

For the 3D photo-reconstruction method at the Santa Cruz site, 515 pictures were taken by hand following a walking itinerary around the gully, with 11 control points deployed on the gully perimeter to facilitate scaling and georeferencing of the resulting model. The large number of photographs reflects a data collection protocol aimed at minimizing the likelihood of missing coverage in some area and maximizing the accuracy of the model (Castillo *et al.*, 2012; James and Robson, 2012). Control point positions were determined by total station. The photographs were processed using structure-from-motion software (PhotoScan v. 0.9.0.1586, Agisoft LLC, Russia) to determine camera characteristics and a sparse 3D point cloud. A dense 3D point cloud was then produced by further processing the results using the dense image matching software PMVS2 (Furukawa and Ponce, 2010; Furukawa *et al.* 2010). An average of ~10 points per cm^2 was obtained. The results were scaled and oriented using a freely available georeferencing application (http://www.lancs.ac.uk/staff/jamesm/software/sfm_georef.htm, James and Robson, 2012) giving horizontal and vertical root mean square errors (RMSEs) on control of 0.016 and 0.036 m, respectively. The results were then interpolated over a 2 cm grid using Surfer (Golden Software Inc, Golden, CO, USA), to obtain a final DEM of the REG.

For the Galapagares area, an airborne campaign was conducted with a 4000 × 3000 resolution digital camera (Panasonic Lumix DMC-GF1 with a 20 mm f/1.7 pancake lens, 40 mm equivalent to 35 mm film format) capturing at f/3.2 and 1/2500 seconds with an angular field of view (FOV) of 47.6° × 36.3° installed on board an aircraft flying at 300 m above ground level. A total of 990 images were taken over a 400-hectares area ensuring a large overlap in the across- and along-track direction of the aircraft. A DEM and orthophotography were obtained through automatic aerial triangulation and camera calibration methods using pix4UAV software (Pix4D SA, Lausanne, Switzerland). Forty control points were measured with dGPS along the study area, mainly at breakpoints associated with man-made infrastructures. A sample of 14 was included during the processing stage for georeferencing the model (0.066 m resolution, 0.087 and 0.23 m horizontal and vertical RMSE, respectively).

For the analysis of the Fuentsanta and Belerda areas, the 5-m-resolution DEM (2010) and orthophotography (2012) available at the Instituto Geográfico Nacional website were employed (CNIG, 2013).

Description of the normalized topographic method

We describe the NorToM through three main aspects: the variables used, GIS processing algorithms and the thresholds required for gully delineation.

Variables in the NorToM

The method is based on two types of variables:

1. Detection variables: normalized slope (NS) and normalized elevation (NE). The objective of these parameters is to detect candidates for gully pixels.
2. Filtering variables: minimum drainage area for gully initiation A_{min}, maximum drainage area for natural stream initiation A_{max}, minimum gully length L_{min}, minimum and maximum gully width W_{min} and W_{max}. They are defined to remove those candidate gully pixels that do not fulfil several topographic gully-related conditions.

Slope and elevation were defined as the detection variables since, morphologically, gullies present steep walls and a flat floor occupying low-elevation positions. Gullies have been defined as steep-walled, poorly vegetated incisions with a small catchment area (Hughes *et al.*, 2001). Since the gully perimeter is the limit between the relatively flat gully margins and the steep gully banks, it is reasonable to use the slope as the key distinguishing factor.

However, an approach based on absolute values is not suitable since the characteristics of the region of change-in-slope at the top of the gully walls might be different between two areas within the same gully or between gullies in different environments. Therefore, a procedure based on variables that are locally based (to capture the topographic variations in the neighbourhood of a particular zone independently on the work extent) as well as statistically relative (applicable to different conditions of slope and elevation) has been followed.

For this purpose, using a similar approach to that commonly applied in statistics to obtain scale-invariant estimates, we normalized the detection variables to obtain a relative index of variation between a pixel and its neighbourhood. The normalized slope NS was defined as:

$$\mathrm{NS} = \frac{S - \overline{S}}{\sigma_s} \qquad (1)$$

where S is the slope of the pixel and $\overline{S}$ and σ_s the mean and standard deviation of the pixel slopes in the neighbourhood defined by a particular window size WS. The normalized slope was used to determine the gully bank candidates using the normalized slope threshold NST.

Likewise, the normalized elevation NE is:

$$\mathrm{NE} = \frac{Z - \overline{Z}}{\sigma_Z} \qquad (2)$$

where Z is the elevation of the pixel and $\overline{Z}$ and σ_Z the mean and standard deviation of the pixel elevations in the neighbourhood. This parameter was employed with two purposes: to detect the gully floor candidates using the lower normalized elevation threshold (LNET) and to remove high elevation areas adjacent to the gully using the upper normalized elevation threshold (UNET).

For gully selection, additional rules must be provided to efficiently differentiate gullies from other landscape elements (filtering variables). Beyond being steep-walled incisions, gullies belong to the drainage network and, therefore, they are located in valley positions. This general condition might be applied in two ways: (i) defining a land stretch along the stream network of a width = W_{max} and removing steep hillslope areas beyond this stretch to facilitate data management (the number of steep areas previously defined by the NST might be large); (ii) to filter out steep hillslope areas close to the gully network (inside the W_{max} stretch) that do not include stream pixels (i.e. less than a minimum length threshold L_{min}).

In addition, two thresholds of drainage area A were defined. A lower limit for gully initiation (A_{min} rule, in line with studies on thresholds for gully initiation) and a higher limit (A_{max} rule) defining the transition from gully to natural streams, i.e. vegetated reaches with minor erosion features. Similar drainage area thresholds for gully detection can be found in the literature [for minimum thresholds (e.g. Daba *et al.*, 2003); for gully-stream limits (for instance, Johansen *et al.*, 2012) using third order channels or (Hughes *et al.*, 2001) $< 10\,\mathrm{km}^2$]. Figure 2 shows a diagram of the main stages of the NorToM and the variables involved.

GIS algorithms in the NorToM

The NorToM was coded as an automated array of ArcGIS™ 9.3 (ESRI Inc., Redlands, CA, USA) algorithms, using Map Algebra syntax for processing speed (Table II). A binary approach is followed, defining candidates to gully areas as pixels of value one and non-gullied areas as zero (Figure 2). Figure 3 visualizes the results from the main processing steps for the Galapagares gully dataset. DEM processing is carried out in the following sequence (Figure 2, Table II):

1. Hydrological analysis: the drainage area and stream network (pixels with a drainage area over A_{min}) are obtained for use in later algorithms.
2. Calculation of DEM slope.
3. Calculation of normalized elevation (Equation (2)).
4. Calculation of normalized slope (Equation (1)).
5. Applying thresholds: NST for gully banks candidates, LNET for gully floor candidates and UNET as a filter for removing high-elevation pixels.
6. Merging the gully banks and gully floor maps to obtain a single gully map.
7. Removing pixels in high-elevation locations.
8. Removing candidate pixels not included inside the stretch of width W_{max} along the stream network. This step eliminates small regions outside the valley locations to accelerate processing.
9. Closing the candidate gully areas to obtain separate regions by the fill-sink algorithm.
10. Removing small hillslope regions which do not fulfil the L_{min} condition, i.e. not including pixels belonging to the stream network.
11. Removing regions beyond the A_{max} threshold that defines the transition between gullies and natural streams.
12. Closing holes. We define a hole as a region sharing all the sides of its perimeter with one-pixel, but with at least one adjacent corner-pixel of value zero. Holes do not verify the sink condition (all cells surrounding a zero region must have a value of one) and are not closed in the first fill-sink operation (Figure 4). The aim of this step is to convert holes at the perimeter into sinks to allow filling. By successively expanding and shrinking one pixel at the gully perimeter, the conversion of holes to sinks is facilitated without modifying the overall gully extent. Closing holes can have a significant impact on the accuracy of the automated method since only one pixel missing may prevent the closing of a region of moderate dimensions. This algorithm (based on an expand-shrink sequence) is

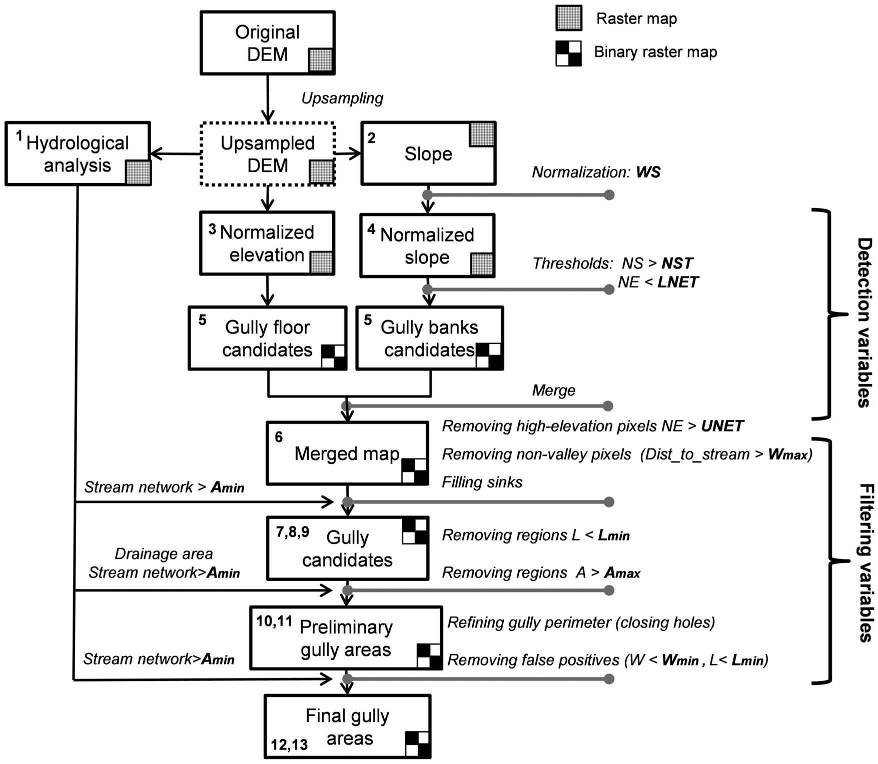

Figure 2. Diagram of the stages and algorithms included in the NorToM. The upsampling process is optional (dotted-line). Steps of the NorToM are indicated on the left corner of the output boxes (correspondence with Table II). A_{min}, minimum drainage area for gully initiation; A_{max}, maximum drainage area for gully-stream transition; L_{min}, minimum gully length; LNET, lower threshold of the normalized elevation; NST, normalized slope threshold; UNET, upper threshold of the normalized elevation; W_{min}, minimum gully width; W_{max}, maximum gully width; WS, window size for the local filter.

performed before removing false positives (shrink-expand sequence) for two reasons: firstly, to prioritize the closing of the gully perimeter that is very vulnerable to edge effects and, secondly, due to the asymmetrical effect of gully delineation (Evans and Lindsay, 2010) that led to higher volume errors for perimeter underestimation than for overestimation.

13. Removing false positives adjacent to the gully. Occasionally, some irregular-shaped areas appear as part of the gullied areas, mainly at headcuts (similar artefacts were reported by Johansen *et al.*, 2012). Normally, actual gully areas and false positives are connected by a narrow 'bridge' (one or two cells wide) of pixels of value one (Figure 4). A shrink operation allows the disconnection of both areas and the later removal of false positives using the L_{min} rule, followed by an expand operation to return the gully limits to its original dimensions. The number of pixels fixed in the shrink operation represents the minimum width of the gully that can be detected since all the gully reaches presenting a width below this limit (whether bridges or actual gully reaches) will be removed.

Optimal thresholds in the NorToM

The key parameters of the NorToM are the window size of the local filter to calculate the mean and standard deviation in the normalization process (WS), and the threshold of the normalized slope (NST).

To assess the effect of WS values relative to the gully size, we evaluated the areal errors in gully perimeter delineation at the REG and PG scales using four different WS values: 1, 1.5, 2 and 3 times W_{max} (with NST set to 0.2). Four indexes of relative areal error were calculated by comparison with the reference measurements: (i) the overestimation error E_o for determining the total area of the estimated gully perimeter exceeding the reference limit; (ii) the underestimation error E_u for calculating the area of the estimated gully perimeter that is inside the reference limit; (iii) the average error E_{av}, for the estimation of the final error summing the E_o and E_u with their respective signs; (iv) the actual error E_{act}, as the sum of the overestimation and underestimation errors in absolute value:

$$E_o = \frac{A_o - A_r}{A_r} \cdot 100 \quad (3)$$

$$E_u = \frac{A_u - A_r}{A_r} \cdot 100 \quad (4)$$

$$E_{av} = \frac{A_c - A_r}{A_r} \cdot 100 \quad (5)$$

$$E_{act} = |E_o| + |E_u| \quad (6)$$

where A_r is the gully area for the reference method and A_c, A_o *and* A_u the total area estimated, overestimated and underestimated by the method under evaluation.

The normalized slope NS presents a natural threshold close to zero: positive NS values correspond to gully wall candidates (steeper pixels than the average) while negative NS values are representative of pixels at the gully margin. In our study, we evaluated the areal errors produced with different positive NST representing increasing margins of safety (0, 0.1, 0.2, 0.3 and 0.5) to find an optimal interval for gully delineation (WS = 2W_{max} in all cases).

Table II. Description of the GIS algorithms applied in the NorToM. The thresholds included in the Map Algebra code must be transformed to the equivalent number of pixels

Stage	Output	Step	Description	Code in Map Algebra	Arc GIS 9.3 Commands
Hydrological analysis	Drainage area streams	1	Calculation of drainage area and stream definition using A_{min}	filldem = fillsink(dem)	*ArcHydroTools/Terrain Procesing/ Dem Manipulation/ FillSinks*
				flowdir = flowdirection (filldem)	*ArcHydroTools/Terrain Procesing/ Flow direction*
				flowacc = flowaccumulation(flowdir)	*ArcHydroTools/Terrain Procesing/ Flow accumulation*
				streamdef = con(flowacc > A_{min}, 1, 0)	*ArcHydroTools/Terrain Procesing/ Stream definition*
Normalization	Normalized variables	2	Calculation of DEM slope	slope = slope (dem, "DEGREE")	*Arctoolbox/ Spatial Analyst tools /Surface/ Slope*
		3	Calculation of normalized elevation	dem_mean = focalmean (dem, rectangle, ***WS***, ***WS***)	*Arctoolbox/Spatial Analyst tools/ Neighbourhood/ Focal statistics*
				dem_std = focalstd (dem, rectangle, ***WS***, ***WS***) norm_elev = (dem - dem_mean) / dem_std	*Spatial Analyst/Raster Calculator*
		4	Calculation of normalized slope	slope_mean = focalmean (slope, rectangle, ***WS***, ***WS***)	*Arctoolbox/Spatial Analyst tools/ Neighbourhood/ Focal statistics*
				slope_std = focalstd (slope, rectangle, ***WS***, ***WS***) norm_slop = (slope - slope_mean) / slope_std	*Spatial Analyst/Raster Calculator*
Applying threshold	Merged map	5	Application of upper and lower thresholds of normalized elevation and threshold of normalized slope	ne_high = con(norm_elev > **UNET**, 0, 1) ne_low = con(norm_elev < **LNET**, 1, 0) ns = con(norm_slop > **NST**, 1, 0)	*Arctoolbox/Spatial Analyst tools/Reclass/ Reclassify*
		6	Obtaining binary map by merging gully floor and bank candidates	merge = ne_low OR ns	*Arctoolbox/Spatial Analyst tools/Math/ Logical/OR*
Selection 1 and closing	Gully candidates	7	Removing pixels in high locations	filter1 = merge * ne_high	*Spatial Analyst/Raster Calculator*
		8	1) Creating a mask adjacent to the stream network; 2) Removing all pixels outside the mask (valley locations)	mask = expand(streamdef, $\boldsymbol{W_{max}}$, list, 1)	*Arctoolbox/Spatial Analyst tools/ Generalization/Expand*
				filter2 = filter1 * mask	*Spatial Analyst/Raster Calculator*
		9	Obtaining closed regions for gully candidates	fillsink1 = fillsink(filter2)	*Arc Hydro Tools/Terrain processing/DEM manipulation/Fill sinks*
Selection 2	Preliminary gully areas	10	1) Defining regions; 2) Calculation of the minimum length of stream inside each region; 3) Removing regions under the threshold	region1 = REGIONGROUP (fillsink1)	*Arctoolbox/Spatial Analyst tools/ Generalization/ Region group*
				sel1 = ZONALSUM(region1, streamdef, DATA)	*Arctoolbox/Spatial Analyst tools/Zonal/ Zonal geometry*
				seldef1 = con((sel1 < $\boldsymbol{L_{min}}$), 0, fillsink1)	*Arctoolbox/Spatial Analyst tools/Reclass/ Reclassify*
		11	1) Defining regions; 2) Calculation of maximum drainage area in each region; 3) Removing regions under the threshold	region2 = REGIONGROUP(seldef1)	*Arctoolbox/Spatial Analyst tools/ Generalization/ Region group*

(*Continues*)

Table 2. (Continued)

Stage	Output	Step	Description	Code in Map Algebra	Arc GIS 9.3 Commands
				sel2 = ZONALMAX(region2, flowacc, DATA)	*Arctoolbox/Spatial Analyst tools/Zonal/ Zonal geometry*
				seldef2 = con((sel2 > $\boldsymbol{A_{max}}$), 0, seldef1)	*Arctoolbox/Spatial Analyst tools/Reclass/ Reclassify*
Refining	Final gully areas	12	1) Expanding gullied areas to include holes; 2) shrinking gullied areas; 3) Filling sinks inside gullied areas	expand1 = expand (seldef2, 1, list, 1)	*Arctoolbox/Spatial Analyst tools/ Generalization/Expand*
				shrink1 = shrink(expand1, 1, list, 1)	*Arctoolbox/Spatial Analyst tools/ Generalization/Shrink*
				fillsink2 = fillsink(shrink1)	*Arc Hydro Tools/Terrain processing/DEM manipulation/Fill sinks*
		13	1) Shrinking gullied areas to break bridges; 2) removing new isolated regions (false positives adjacent to the gully) using L_{min}; 3) Expanding gullied areas without false positives	shrink2 = shrink(fillsink2, $\boldsymbol{W_{min}}$, list, 1)	*Arctoolbox/Spatial Analyst tools/ Generalization/Shrink*
				region3 = REGIONGROUP (shrink2)	*Arctoolbox/Spatial Analyst tools/ Generalization/ Region group*
				sel3 = ZONALSUM(region3, streamdef)	*Arctoolbox/Spatial Analyst tools/Zonal/ Zonal geometry*
				seldef3 = con((sel3 < $\boldsymbol{L_{min}}$), 0, shrink2)	*Arctoolbox/Spatial Analyst tools/Reclass/ Reclassify*
				gully = expand(seldef3, $\boldsymbol{W_{min}}$, list, 1)	*Arctoolbox/Spatial Analyst tools/ Generalization/Expand*

Note: A_{min}, minimum drainage area for gully initiation; A_{max}, maximum drainage area for gully-stream transition; L_{min}, minimum gully length; LNET, lower threshold of the normalized elevation; NST, normalized slope threshold; UNET, upper threshold of the normalized elevation; W_{min}, minimum gully width; W_{max}, maximum gully width; WS, window size for the local filter.

Comparison between the field reference and NorToM at the REG and PG scales

We evaluated the impact of DEM resolution on the accuracy of areal and volume estimates of gully erosion in two situations: (i) when the original resolution is downsampled to coarser pixel sizes to simulate decreasingly data quality; (ii) when an available resolution is upsampled to finer pixel sizes in an attempt to increase accuracy.

Resolution influence: downsampling original resolutions

At the REG scale, we assessed the areal errors of the NorToM by considering four DEM resolutions: 2, 5, 10 and 20 cm. The coarser resolutions were obtained by downsampling the original 2-cm DEM using the cubic resampling method. A similar methodology was followed by Wu *et al.* (2008a) to assess the influence of resolution on hydrologic application. Likewise, at the PG scale, a series of DEM resolutions (0.12, 0.25, 0.5, 1.0 and 2.0 m) was produced by resampling the 6.6-cm original DEM. In this case, the original resolution was not included in the analysis due to the time-consuming processing of the NorToM for such a large dataset. All the NorToM runs were performed using a WS twice W_{max}, NST = 0.2, LNET = −1 and UNET = 0.2. The downsampled resolutions were indicated placing a d prefix before the cell size, e. g. d2m for the 2-m resolution from the original 0.066 m DEM. We also evaluated the performance of the manual digitation method (MDM) at the REG and PG scales, prior to its use as a comparison at larger scales (see later). The MDM is based on the manual delineation of the gully perimeter by distinguishing visually the change in slope at the top of the gully walls on a slope map using GIS. The MDM has been used as a comparison dataset in previous works (Evans and Lindsay, 2010; Perroy *et al.*, 2010; Shruthi *et al.*, 2011).

For volume calculations, we applied a similar routine to that employed by Daba *et al.* (2003): (i) gully perimeter delineation by the NorToM; (ii) conversion of the gully perimeter vertices to *x-y* points; (iii) extracting DEM values to obtain point elevations; (iv) interpolation of the gully lid surface using point elevations (inverse-distance-weighed method); (v) extracting the gully lid and DEM surfaces using the perimeter as a mask; (vi) estimating the volume between the two surfaces using the cut-and-fill algorithm.

The reference volume V_r resulted from the calculation of the volume enclosed between a reference gully lid and the reference DEM. The reference DEM was considered to be the gully surface obtained using the finest resolution available (2 cm and 6.6 cm for REG and PG, respectively). The reference gully lid was defined by interpolating a surface using the coordinates of the reference field dataset (either total station or dGPS). We evaluated the volume difference D_v between V_r and the calculated volume for a particular method V_i using Equation (7):

$$D_v = \frac{V_i - V_r}{V_r} \cdot 100 \tag{7}$$

In order to assess the impact of DEM resolution on volume estimates independently from the influence of gully delineation inaccuracy, we carried out an analysis of the volume differences using the reference gully perimeter derived from the field measurements. For this purpose, we considered the reference gully lid as a

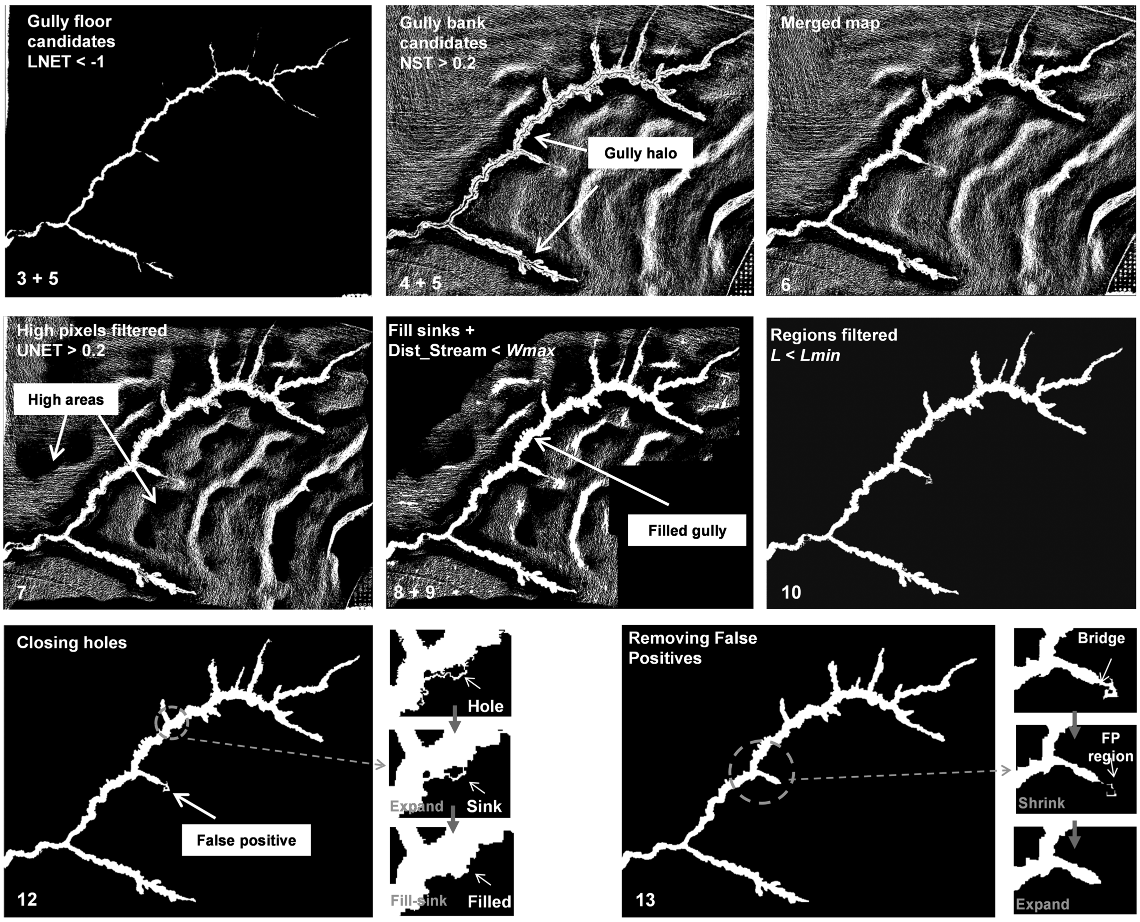

Figure 3. Visual outline of the normalized topographic method. On the bottom left corner, the step number (Table II) is shown. FP, false positive; L_{min}, minimum gully length; LNET, lower threshold of the normalized elevation; NST, normalized slope threshold; UNET, upper threshold of the normalized elevation.

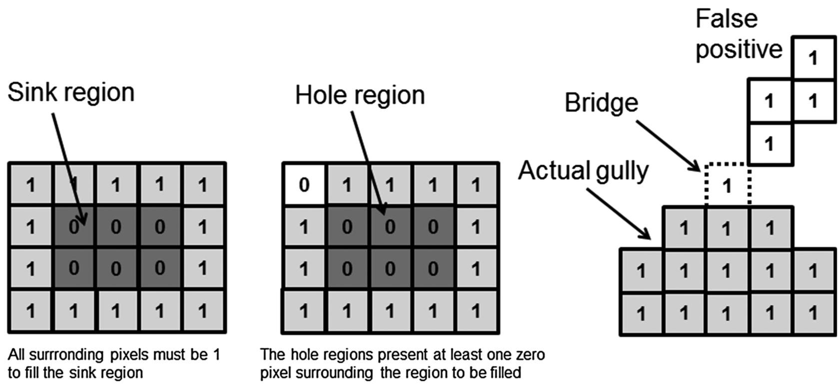

Figure 4. Sketch of the main features involved in the refining stage of NorToM. 1: candidate to gully pixel; 0: non-gully pixel.

fixed surface and we used decreasing DEM resolutions (the same range used in the areal error assessment). This analysis provided an evaluation of the degradation of volume estimates as a function of the DEM quality with no errors involved in gully delineation.

Finally, the volume differences for the NorToM were calculated. These deviations from V_r included the impact of the inaccuracy in gully delineation using the automated procedure. In all cases, the gully lid and gully DEM were obtained by resampling the resolution under evaluation to the finest pixel size (2 cm and 12 cm) in order to minimize the errors in the conversion from feature (gully perimeter) to raster data (gully lid surface).

Resolution influence: upsampling available resolutions for operational purposes

As a consequence of working with raster data, the accuracy of gully delineation is sensitive to DEM cell size. For coarse resolutions, the exclusion of a single cell might lead to a significant error in the gully perimeter. These errors propagate in volume calculations because an underestimation of the gully limits produces not only a decrease of the gully lid area but also a reduction of the gully lid elevation. Low resolutions also decrease the efficiency of several automated algorithms such as the fill-sink or refining operations, potentially resulting in large regions not being filled and greater underestimation. These errors can be reduced by upsampling the original coarse DEM resolution to finer cell sizes. This approach does not result in improved data quality (the new cell values are calculated from that of the original cell, not providing additional topographic information) but has advantages in terms of reducing the magnitude of the edge effects in the automated procedure. We assessed the influence of upsampling (cubic resampling) on areal and volume deviations from the field reference when coarse DEM resolutions were used (10 cm and 20 cm and 1 m and 2 m, at the REG and PG scales, respectively). The upsampled resolutions were indicated placing the up prefix before the final cell size, e.g. d2up0.5 m indicating a final 0.5 m resolution obtained from the previously downsampled 2-m resolution.

Comparison between NorToM and MDM at the LG and BL scales

At the LG and BL scales we compared the NorToM performance with results from the MDM, because no field measurements were available. The differences between MDM and NorToM (D_u, D_o, D_{av} and D_{act} in gully delineation and D_v for volume estimates) were calculated following the same approach used at the REG and PG scales, in this case taking the MDM as the reference. For the Fuentsanta site, the NorToM parameters were: WS = 800 m ($2W_{max}$), NST = 0.2, LNET = −1, UNET = 0.5, A_{min} = 1 km^2, A_{max} = 25 km^2, L_{min} = 100 m, W_{max} = 400 m, W_{min} = 10 m. As for the Belerda area, two sequential applications of the NorToM (WS equal to 500 m and 2000 m) were necessary due to the significant variations in dimensions between the main and secondary branches. Parameter used were: NST = 0.2, LNET = −1, UNET = 0.5, A_{min} = 4 km^2, A_{max} = 50 km^2, L_{min} = 100 m, W_{max} = 250 and 1000 m, W_{min} = 10 m.

Results

Optimal thresholds in NorToM

Figure 5 shows the areal errors produced in gully delineation for increasing WS and NST for the NorToM. The WS analysis showed minimum errors at WS = 3 m for REG, i.e. 1.5 times W_{max} (E_{act} = 16.8%), and 40 m for the PG scale, twice W_{max} (E_{act} = 10.8%). In both cases, lower WS values led to underestimation of the gully area (negative E_{av}) and larger values to overestimation, as well as to longer processing times.

At REG scale, NST = 0.3 minimized the errors produced (E_{act} = 17.8%, E_{av} = 0.8%) whereas, in the PG case, the minimum actual error was found over the 0.1–0.3 interval (E_{act} ≈ 10.8%). In the subsequent NorToM analyses, WS = $2W_{max}$ and NST = 0.2 were chosen.

We used a LNET value of −1 (i.e. selecting only pixels with elevations deviations below −1σ) to determine gully floor candidates with a wide margin of safety to avoid interfering gully delineation by the NS. Finally, we applied a UNET of 0.2 to remove high elevation areas, again, for safety considerations (gully areas present lower elevations than the average, i.e. negative NE values). At the large gully and badland scale, an UNET value of 0.5 was used, since at several locations the UNET selection was more stringent than the NST. This is a consequence of the compact geometry of the gully networks, with main and secondary gully branches bunching together. This resulted in a WS being included inside gullied areas so that a small amount of non-gullied areas were considered in the normalization process.

Comparison between the field reference and NorToM at the REG and PG scales

Charts on the left side of Figure 6 show the areal errors produced in gully delineation in the NorToM for decreasing resolutions (left side of the chart) and after the upsampling operation (right side). Comparable results were obtained for a range of small to medium resolutions: E_{act} around 19 % from 2 cm to d5cm in REG and E_{act} close to 11% from d0.12 m to d0.5 m for the PG scale. In these cases, the average error was <5 %. For coarser resolutions, increasing errors were found with maximum E_{act} values >30% for d20cm and d2m. When

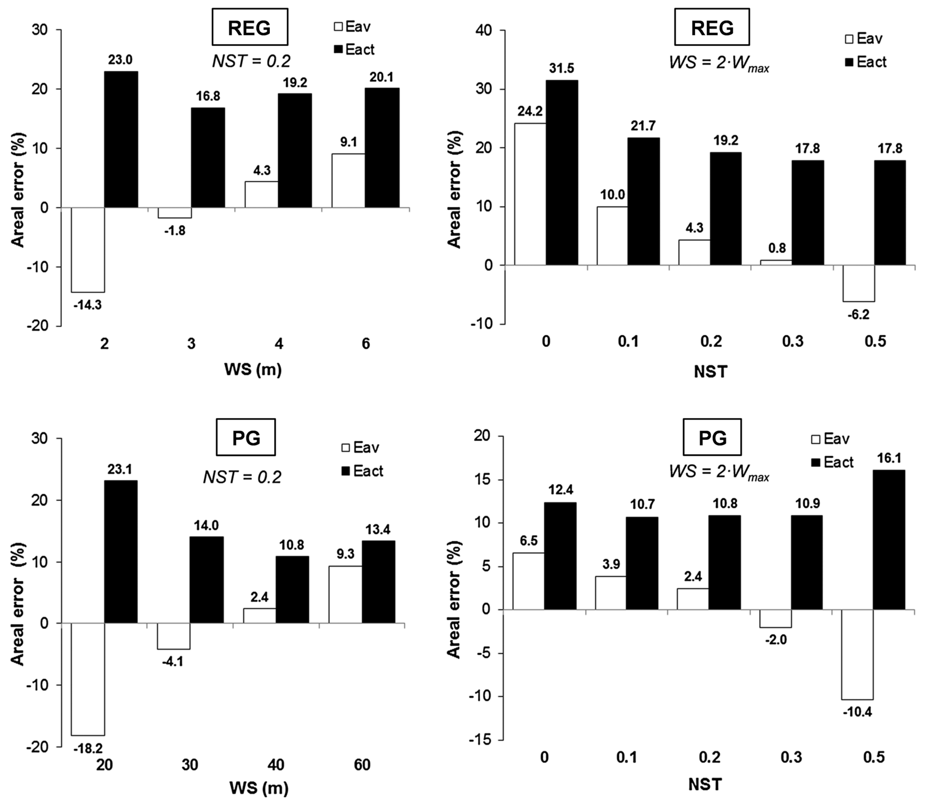

Figure 5. Error assessment in gully delineation as a function of the window size (WS) and the normalized slope threshold (NST) in NorToM at the rill-ephemeral gully (REG) and permanent gully (PG) scales. E_{act}, actual error (%); E_{av}, average error (%).

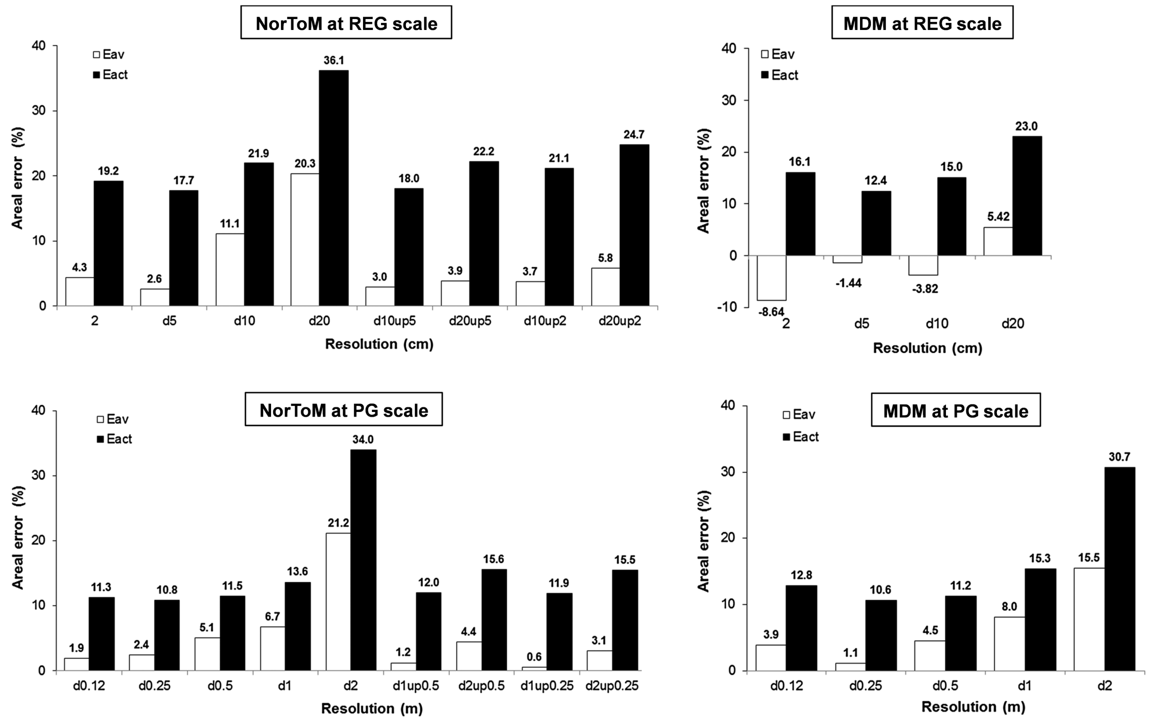

Figure 6. Error assessment in gully delineation as a function of resolution for NorToM and MDM at the REG and PG scales. MDM, manual delineation method; E_{act}, actual error (%); E_{av}, average error (%).

upsampling was applied in the NorToM (on the right side of each chart), a significant reduction of areal errors was obtained (i.e. for d20up5cm, E_{act} moved from 36.1% to 22.2% at the REG scale and, for d2up0.5 m, from 34.0% to 15.6% for the PG), with a much more gradual degradation of errors with increasing resolutions. Moreover, the differences in areal errors between the two cell sizes chosen in the upsampling process were not significant. At the REG scale, E_{act} was around 20% for d10up2cm and d10up5cm whereas close to 23% for resolutions d20up2cm and d20up5cm. For the PG case, E_{act} was close to 12% for 1 m and 15.5% for 2 m using 0.25 and 0.5 m as final pixel sizes.

The MDM produced slightly better estimates than the NorToM at the REG scale (minimum $E_{act} = 12.4$ %) and provided very similar results at the PG scale (on the right side of Figure 6).

Figure 7 shows the volume deviations from V_r produced using the reference perimeter and the NorToM perimeter at the REG and PG scales as a function of resolution. For the first case, decreasing resolutions produced small and slightly increasing underestimation errors, with a maximum volume error

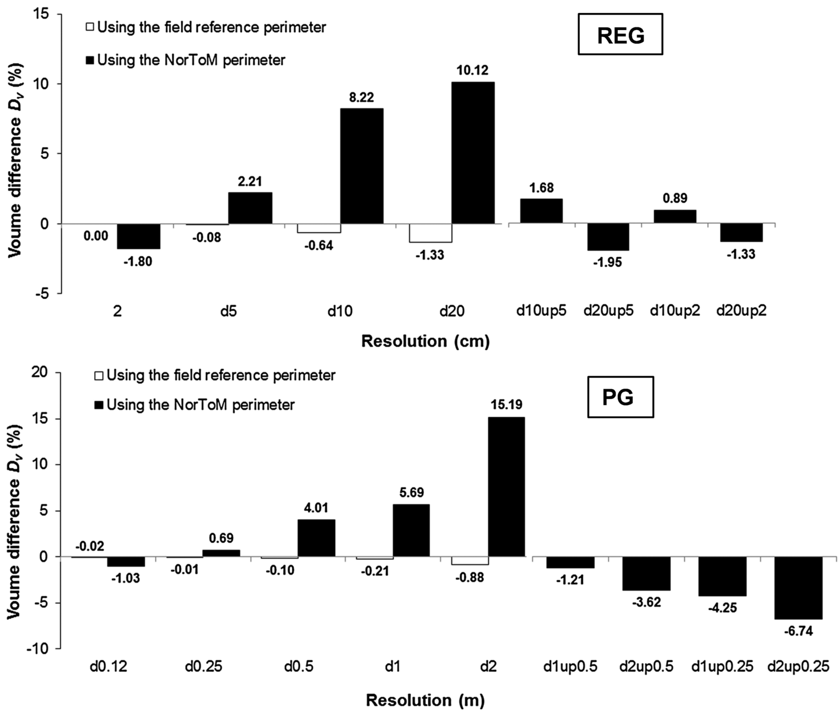

Figure 7. Volume differences between the reference volume and the volume estimates obtained using the reference and the NorToM perimeters as a function of resolution at the rill-ephemeral gully (REG) and permanent gully (PG) scales.

of −1.33% and −0.88%, for REG and PG, respectively. Regarding the NorToM, a tendency towards volume overestimation for increasing cell sizes was found. The maximum volume difference was found at the coarsest resolutions and was >10 % in both cases. Volume deviations were reduced when upsampling was carried out (<7% in absolute value in all cases, bars on the right side of Figure 7) and the differences between cell sizes were not significant.

Comparison between NorToM and MDM at the LG and BL scales

Figure 8 shows the areal and volume differences when the NorToM and MDM results were compared. At the Fuentsanta and Belerda sites, D_{act} was larger (~24%) than those obtained at the smaller scales (17.07 and 13.63% at the REG and PG scales, respectively, given for comparison on the left side of the figure), although the average differences between both methods remained small (<6 % in absolute value). As for the volume differences D_v, a maximum value close to −20% was obtained at the Belerda site, considerably greater than for the rest of the cases.

Discussion

Evaluation of the NorToM

There are a number of advantages in using the NorToM. Firstly, it makes use of a group of variables readily available from a DEM. In other studies based on object-oriented classification (Eustace *et al.*, 2011; Shruthi *et al.*, 2011), for instance, spectral characteristics of the images were required. In addition, the NorToM rule-set includes topographic variables linked directly to gully morphological features that, in fact, have been used in the literature to define these landforms. The threshold values for the filtering variables are not critical and can be determined with a wide safety of margin to ensure no gully is left out in the process. Note that these variables only operate once candidate regions are formed by the detection variables, so are not defining gully presence but filtering the regions already detected.

Secondly, the NorToM defines the gully limits explicitly by using the contrast in slope between the margins and the gully. It detects a sharp, not gradual, change in normalized slope and provides an efficient approach to outlining gullied areas (see the 'gully halo' in Figure 3, with the white steep gully banks surrounded by a black stretch of flat gully margins). In our study, use of the NS proved to be more efficient for gully delineation than NE (a parameter related to the difference from mean elevation DFME used in Evans and Lindsay, 2010) because the slope is the critical factor differentiating the steep gully banks from the relatively flat gully floor and gully margins. In those studies based on object-oriented approaches for gully mapping, it is not straightforward to identify which criterion was actually applied to define the gully perimeter by looking at the rule-set provided (Eustace *et al.*, 2011; Shruthi *et al.*, 2011; Johansen *et al.*, 2012).

Thirdly, the threshold definition for gully detection in the NorToM represents a scale-independent approach: (i) spatially, because a local filter is applied; (ii) in terms of value scale, due to the normalization process. Thus, the NorToM was intended to be more flexible and applicable to different gully landscapes than those approaches based on absolute thresholds, since the threshold remained unchanged regardless the dimensions of erosion features. Evans and Lindsay (2010) used the DFME index (threshold value −0.25 m) and the positive plan curvature (5° m^{-1}). Eustace *et al.* (2011) employed several rules simultaneously, such as mean slope (15°), mean standard deviation of DEM (50 m^2) or mean standard deviation of slope (6°). All of these thresholds are not relative and will likely depend on the characteristics of the study area.

Finally, the NorToM presents several algorithms for refining gully delineation and obtaining separate polygons for each gully. This step greatly facilitated the assessment of the geometry of gully areas and volume calculations. We employed, for the first time, a fill-sink algorithm to obtain a preliminary gully area, a closing-hole algorithm to improve the delineation at the top of the gully walls, and a breaking-bridges sequence to remove false positives. These tools were useful to attain a single continuous polygon while, simultaneously, reducing the amount of error at the gully rims. These NorToM features made it applicable to multiple-gully landscapes such as the Galapagares area (Figure 1b) comprising separate small- to medium-sized gully networks. Separate gully polygons were obtained, with no apparent errors in the gully perimeter. Higher resolutions implied more accurate gully detection due to its superior ability to delineate the narrower reaches within the gully networks. At the landscape scale, the definition of the optimal window size and resolution should take into consideration the minimum width of the erosion features to be detected within the study area.

Some limitations of the NorToM must be noted. Firstly, it depends on the normalization of the detection variables on a local basis (defined by the WS) which can be a time-consuming process for fine resolutions at large scales. The processing time for the normalization process depends on the total number of pixels involved in the operations (n_{pixels}) and the computing power:

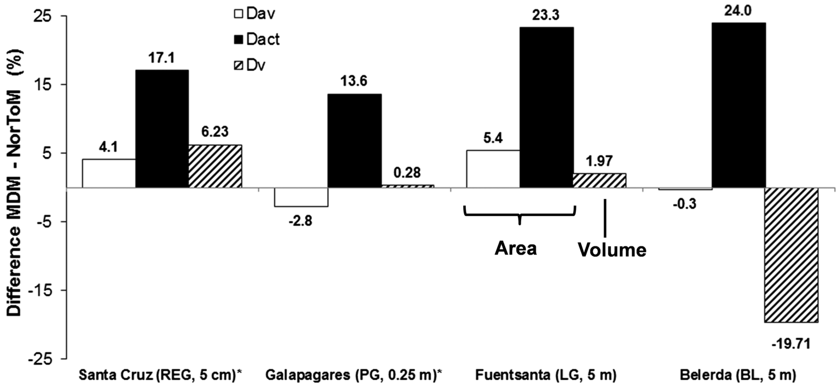

Figure 8. Areal and volume differences between the manual delineation method (MDM, as the reference) and the NorToM at the large gully (LG) and badland (BL) scales. The differences for the REG and PG scales are given for comparison purposes (*). D_{act}, actual difference; D_{av}, average difference; D_v, volume difference.

$$t_{\text{norm}} \approx n_{\text{pixels}} \times t_{\text{unit}} = 4\,\frac{\text{extent}(\text{m}^2)\cdot \text{WS}^2(\text{m})}{\text{resolution}^4(\text{m})} \times t_{\text{unit}} \qquad (8)$$

where t_{norm} stands for the processing time for the normalization stage, n_{pixels} for the number of pixels, four is the number of filtered maps required in the NorToM (mean and standard values of elevation and slope), the extent is the total area of the landscape considered, WS is the dimensions of the filter window and t_{unit} the processing time per pixel included in the operations.

In our study, an average processing time for the normalization process of ~7 ms per million pixels was found. For instance, for the computer used in this study (intel Core i7 2Ghz, 8 GB RAM), the normalization process would take ~13 hours for a 0.25-m resolution, 40-m WS, in a 400-ha landscape window (a total of 160 × 160 pixels in each pixel neighbourhood, 64 million pixels throughout the study area). Although in Figure 2 the upsampling process has been included as an optional first stage for clarity, it is worth nothing: (i) this is only a recommended step when only coarse resolution DEMs are available; (ii) it might be applied after the normalization process (the most time-consuming step), since it yields benefits at the fill-sink and refining operations. Computing constraints will be reduced in the future as technology advances but currently they must be considered a limitation for automated gully mapping of extensive areas.

In addition, as the NorToM requires the definition of a window of constant dimensions, landscapes with highly contrasting gully widths might require the use of several runs with different WS to allow a more precise characterization of the varying gully geometry (see later).

Optimal thresholds in the NorToM

We found that approximately 1.5–2 times W_{max} was an optimal interval for WS. This range of sizes turned out to be suitable since they allowed the inclusion of a significant and balanced amount of gully and non-gully pixels inside the filter window for comparison purposes. Evans and Lindsay (2010) employed a filter size equal to W_{max} in the Bleaklow Plateau (30 m), although they recognized that this size might not be sufficient. In this case, the proportion of non-gully pixels might not be sufficiently representative at some locations and the application of the close-to-zero threshold might lead to discarding pixels belonging to the gully. Careful attention must be paid to resolution and WS in order to find a trade-off between accuracy and time requirements (Equation (8)).

Additionally, the results showed that the areal errors were not very sensitive to the NET, provided that the threshold is maintained between 0.1 and 0.3. A LNET value of −1 was satisfactory for detecting the gully floor without affecting the detection of the gully limits by NET. A UNET of 0.2 is recommended for gullies with separate branches but, if the network is very compact, larger values are advisable (e.g. 0.5). Although the use of the UNET filter is not critical for gully delineation, we found it useful in certain cases to remove false positives at the gully perimeter. For instance, two olive mounds (steep and high-elevation pixels) adjacent to the REG were almost completely eliminated after applying this filter, as well as sparse high-standing vegetation at the gully rims at the PG scale.

Comparison between the field reference and NorToM at the REG and PG scales

The NorToM performed similarly to the MDM at the REG and PG scales. The slightly larger errors at the REG scale are a consequence of the challenging geometry of the selected REG and its higher sensitivity to minor field elements such as stones, vegetation and micro-topography (note that the average depth of the REG was 20 cm).

DEM resolution played an important role in the delineation accuracy with the NorToM when upsampling was not performed. We found that as long as the resolution is <10% W_{av}, the areal errors were not greatly affected. Nevertheless, by using the upsampling process in the NorToM, we found that areal errors can be reduced to two thirds or even to half the original value for the coarsest resolutions. Consequently, the original data resolution requirements might be reduced to 10% W_{max} or 20% W_{av}, with the final upsampled resolution set to a value around 5% W_{av}.

These results open the door to defining optimal approaches for gully assessment in advance so that errors and processing times are kept at a minimum. It also demonstrates that despite the fact that the resolution of conventional datasets (usually 5–10 m) are only suitable for the assessment of large gully systems, the increasingly available high-resolution products might offer an excellent opportunity for the accurate evaluation of medium-sized gullies using automated approaches.

For the analysis of gully volume, resolution was found to exert little influence on volume calculations if there were no errors in the gully perimeter. The most significant part of the volume error is derived from inaccurate gully delineation. The NorToM volume estimates showed deviations which remained fairly constant up to medium resolutions, but became large for coarse resolutions. In these cases, the upsampling process, as for gully delineation, was successful in reducing volume errors.

Comparison between NorToM and MDM at the LG and BL scales

The performance of the NorToM was satisfactory for the Fuentsanta and Belerda areas, but the areal differences were higher than those produced at smaller scales. At the Fuentsanta large gully system, the surrounding structure of man-induced land-uses (urbanizations, industrial areas, cereal plots, road infrastructures) complicated automated delineation. For the Belerda site, two consecutive analyses were required (WS equal to 500 m and 2000 m) to capture the contrasting dimensions of the gully channels at this scale. Both outcomes were merged into a single map using a logical OR operation. This sequential approach was satisfactory at the scale under study (12 km × 12 km window extent, covering two barrancos), but it may present limitations if a larger scale is addressed. If we take the badland system as a whole, the NorToM would not be efficient in mapping the complete network. For instance, the definition of the headwaters of the network is an arduous task, since the channels are surrounded by very steep hillslopes, making the normalized slope of little use as a detection variable. Moreover, the variation in gully dimensions is extreme, ranging from several metres at the headwaters to several kilometres at the middle reaches, accentuating the difficulties concerning the WS definition. In fact, not only methodological aspects are involved here, but also geomorphological issues regarding the very definition of a badland area.

Conclusions

We have described and tested a normalized topographic method for gully mapping using topographic data in a variety of scales ranging from the rill to the badland landscape. This study demonstrates that using the normalized elevation and slope as detection variables, a group of topographic variables for selection purposes in conjunction with an array of automated GIS algorithms was an efficient and scale-independent approach for gully mapping. The optimal window size and normalized slope thresholds were in the order of twice the maximum width of the gully and 0.2, respectively. The NorToM provided a good approximation to the reference datasets in gully area and volume at the rill and gully scales for a range of resolutions, provided that upsampling was carried out for the coarsest DEM resolutions. We found optimal DEM resolutions and upsampled pixel sizes of approximately 20% and 5% of the mean gully width, respectively.

For the large gully and badland scales, the areal and volume estimates of the NorToM were in line with those obtained using the MDM, although the differences increased in complex gully systems (due to surrounding patterns of anthropogenic land-use and extreme topographical variations). At the badland site, two sequential NorToM runs using different window sizes were required to adapt the method to the contrasting dimensions of the gully network. Since the NorToM was successfully applied to different scales and environments and its main explanatory variables are based on local and relative topographical analysis, it is believed to be applicable to a wide range of situations. Nevertheless, its application might be limited in those contexts in which there is little contrast in slope between the margins and the gully channel or extreme differences in gully dimensions typical of badland landscapes.

Acknowledgements—This study was supported by Projects P08-AGR-03925 (Andalusian Government) and AGL2009-12936-C03-01 (Spanish Ministry of Science and Innovation), AGL2012-40128-C03-01 (Spanish Ministry of Economy and Competitiveness), RESEL (Spanish Ministry for Environment and Rural and Marine Affairs) and FEDER funds. This support is gratefully acknowledged. The authors would like to thank A. Gomez, D. Notario, A. Vera, A. Hornero, and R. Romero (QuantaLab-IAS-CSIC research laboratory) for their contributions to the airborne and field campaigns. The authors would also like to thank the reviewers for their comments and suggestions that helped to improve the manuscript.

Nomenclature

A_c	=	gully area calculated by the selected method
A_o	=	area overestimated in the reference gully area
A_r	=	the reference gully area
A_u	=	area underestimated in the reference gully area
A_{max}	=	maximum drainage area defining the transition from gully to natural streams
A_{min}	=	minimum drainage area for gully initiation
DEM	=	digital elevation model
D_{act}	=	actual difference (%)
D_{av}	=	average difference (%)
D_v	=	volume difference (%)
E_{act}	=	actual error (%)
E_{av}	=	average error (%)
E_o	=	overestimation error (%)
E_u	=	underestimation error (%)
E_v	=	volume error (%)
H_{av}	=	average gully depth
L_{min}	=	minimum gully length
MDM	=	manual delineation method
NE	=	normalized elevation
NET	=	normalized elevation threshold
NS	=	normalized slope
NST	=	normalized slope threshold
NorToM	=	normalized topographic method
V_i	=	gully volume calculated using a DEM of a particular resolution
V_r	=	reference volume
W_{av}	=	average gully width
W_{max}	=	maximum gully width
WS	=	window size of the local filter

References

Casalí J, López JJ, Giráldez JV. 1999. Ephemeral gully erosion in southern Navarra (Spain). *Catena* **36**: 65–84.

Casalí J, Loizu J, Campo MA, De Santisteban LM, Álvarez-Mozos J. 2006. Accuracy of methods for field assessment of rill and ephemeral gully erosion. *Catena* **67**: 128–138.

Castillo C, Perez R, James MR, Quinton JN, Taguas EV, Gómez JA. 2012. Comparing the accuracy of several field methods for measuring gully erosion. *Soil Science Society of America Journal* **76**: 1319–1332.

CNIG, Centro Nacional de Descargas, Instituto Geográfico Nacional. 2013. https://www.cnig.es [November 2013].

Daba S, Rieger W, Strauss P. 2003. Assessment of gully erosion in eastern Ethiopia using photogrammetric techniques. *Catena* **50**: 273–291.

De Santisteban LM, Casalí J, López JJ. 2006. Assessing soil erosion rates in cultivated areas of Navarre (Spain). *Earth Surface Processes and Landforms* **31**: 487–506.

Eustace AH, Pringle MJ, Denham RJ. 2011. A risk map for gully locations in central Queensland, Australia. *European Journal of Soil Science* **62**: 431–441.

Evans M, Lindsay J. 2010. Quantifying gully erosion in upland peatlands at the landscape scale. *Earth Surface Processes and Landforms* **35**: 876–886.

Furukawa Y, Curless B, Seitz SM, Szeliski R. 2010. Towards internet-scale multi-view stereo. *Computer Vision and Pattern Recognition* 1434–1441. DOI. 10.1109/CVPR.2010.5539802

Furukawa Y, Ponce J. 2010. Accurate, dense, and robust multiview stereopsis. *IEEE Transactions on Pattern Analysis and Machine Intelligence* **32**: 1362–1376. DOI. 10.1109/TPAMI.2009.161

Giménez R, Marzolff I, Campo MA, Seeger M, Ries JB, Casalí J, Álvarez-Mozos J. 2009. Accuracy of high-resolution photogrammetric measurements of gullies with contrasting morphology. *Earth Surface Processes and Landforms* **34**(14): 1915–1926.

Gómez-Gutiérrez A, Schnabel S, Lavado-Contador F. 2009. Gully erosion, land use and topographical thresholds during the last 60 years in a small rangeland catchment in SW Spain. *Land Degradation and Development* **20**: 535–550.

Hancock GR. 2005. The use of DEMs in the identification and characterization of catchment over different grid scales. *Hydrological Processes* **19**: 1727–1749.

Hughes AO, Prosser IP, Stevenson J, Scott A, Lu H, Gallant J, Moran CJ. 2001. Gully Erosion Mapping for the National Land and Water Resources Audit, Technical Report 26/01. CSIRO Land and Water: Canberra. http://www.clw.csiro.au/publications/technical2001/tr26-01.pdf [October 2013].

James LA, Watson DG, Hansen WF. 2007. Using LiDAR data to map gullies and headwater streams under forest canopy: South Carolina, USA. *Catena* **71**: 132–144.

James M, Robson S. 2012. Straightforward reconstruction of 3d surfaces and topography with a camera: accuracy and geoscience application. *Journal of Geophysical Research* **117**: 17.

Johansen K, Taihei D, Tindall D, Phinn S. 2012. Object-based monitoring of gully extent and volume in North Australia using LiDAR data. *Proceedings of the 4th GEOBIA, May 2012*, Brazil, 168.

Martínez-Casasnovas JA, Ramos MC, Ribes-Dasi M. 2002. Soil erosion caused by extreme rainfall events: mapping and quantification in agricultural plots from very detailed digital elevation models. *Geoderma* **105**: 125–140.

Marzolff I, Ries JB, Poesen J. 2011. Short-term versus medium-term monitoring for detecting gully-erosion variability in a Mediterranean environment. *Earth Surface Processes and Landforms* **36**: 1604–1623.

Perroy RL, Bookhagen B, Asner G, Chadwick O 2010. Comparison of gully erosion estimates using airborne and ground-based LiDAR on Santa Cruz Island, California. *Geomorphology* **118**: 288–300.

Poesen J, Nachtergaele J, Verstraeten G, Valentin C. 2003. Gully erosion and environmental change: importance and research needs. *Catena* **50**: 91–133.

Shruthi R, Kerle N, Jetten V. 2011. Object-based gully feature extraction using high spatial resolution imagery. *Geomorphology* **134**: 260–268.

Thompson J, Bell J, Buttlet CA. 2001. Digital elevation model resolution: effects on terrain attribute calculation and quantitative soil-landscape modeling. *Geoderma* **100**: 67–89.

Wu S, Li J, Huang GH. 2008a. A study on DEM-derived primary topographic attributes for hydrologic applications: sensitivity to elevation data resolution. *Applied Geography* **28**: 210–223.

Wu Y, Zheng Q, Zhang Y, Liu B, Cheng H, Wang Y. 2008b. Development of gullies and sediment production in the black soil region of northeastern China. *Geomorphology* **101**: 683–691.

Zandbergen PA. 2006. The effect of cell resolution on depressions in digital elevation models. *Applied GIS* **2**(1): 04.1–04.35.

Zhang W, Montgomery DR. 1994. Digital elevation model grid size, landscape representation and hydrologic simulations. *Water Resources Research* **30**(4): 1019–1028.